A High Yield of New Sightlines for the Study of Intergalactic Helium: Far-UV-Bright Quasars from SDSS, GALEX, and HST^1

David Syphers², Scott F. Anderson³, Wei Zheng⁴, Daryl Haggard³, Avery Meiksin⁵, Kuenley Chiu⁶, Craig Hogan³, Donald P. Schneider⁷, Donald G. York^{8,9}

ABSTRACT

Investigations of He II Ly α (304 Å rest) absorption toward a half-dozen quasars at $z\sim 3-4$ have demonstrated the great potential of helium studies of the IGM, but the current critically small sample size of clean sightlines for the He II Gunn-Peterson test limits confidence in cosmological inferences, and a larger sample is required. Although the unobscured quasar sightlines to high redshift are extremely rare, SDSS DR6 provides thousands of z>2.8 quasars. We have cross-correlated these SDSS quasars with GALEX GR2/GR3 to establish a catalog of 200 higher-confidence (\sim 70% secure) cases of quasars at z=2.8-5.1 potentially having surviving far-UV (restframe) flux. We also catalog another 112 likely far-UV-bright quasars from GALEX cross-correlation with other (non-SDSS) quasar compilations. Reconnaissance UV prism observations with HST of 24 of our SDSS/GALEX candidates confirm 12 as detected in the far-UV,

¹Based on observations with the NASA/ESA Hubble Space Telescope obtained at the Space Telescope Science Institute, which is operated by the Association of Universities for Research in Astronomy, Incorporated, under NASA contract NAS5-26555.

²Physics Department, University of Washington, Seattle, WA 98195; dsyphers@phys.washington.edu

³Astronomy Department, University of Washington, Seattle, WA 98195; anderson@astro.washington.edu

 $^{^4\}mathrm{Department}$ of Physics and Astronomy, Johns Hopkins University, Baltimore, MD 21218; zheng@pha.jhu.edu

⁵Scottish Universities Physics Alliance (SUPA), Institute for Astronomy, University of Edinburgh, Royal Observatory, Edinburgh EH9 3HJ, United Kingdom

⁶Anglo-Australian Observatory, Epping, NSW 1710, Australia

 $^{^7 \}mathrm{Pennsylvania}$ State University, Department of Physics & Astronomy, 525 Davey Lab, University Park, PA 16802

 $^{^8\}mathrm{Department}$ of Astronomy and Astrophysics, The University of Chicago, 5640 South Ellis Avenue, Chicago, IL 60637

⁹Enrico Fermi Institute, University of Chicago, 5640 South Ellis Avenue, Chicago, IL 60637

with at least 9 having flux extending to very near the He II break; with refinements our success rate is even higher. Our SDSS/GALEX selection approach is thereby confirmed to be an order of magnitude more efficient than previous He II quasar searches, more than doubles the number of spectroscopically confirmed clean sightlines to high redshift, and provides a resource list of hundreds of high-confidence sightlines for upcoming He II and other far-UV studies from HST. Our reconnaissance HST prism spectra suggest some far-UV diversity, confirming the need to obtain a large sample of independent quasar sightlines across a broad redshift range to assess such issues as the epoch(s) of helium reionization, while averaging over individual-object pathology and/or cosmic variance.

Subject headings: catalogs — galaxies: active — intergalactic medium — quasars: general — surveys — ultraviolet: galaxies

1. Introduction

A substantial fraction (perhaps most) of the baryons in the Universe did not collapse into such dense structures as stars, galaxies, and quasars, instead remaining behind in a more dilute intergalactic medium (hereafter, IGM), composed primarily of primordial hydrogen and helium (e.g., see recent review by Meiksin 2008). Ultraviolet radiation from massive early stars, star-forming galaxies, and quasars gradually reionized their surrounding IGM, ultimately ending the "dark ages". Cosmic microwave background studies provide one important indirect chronometer for reionization: the Wilkinson Microwave Anisotropy Probe (WMAP) 5-year data (Dunkley et al. 2008) constrain sudden one-time hydrogen reionization to z > 6.7 at 3σ , and place it at $z = 11.0 \pm 1.4$ (1σ). However, the WMAP measures do not strongly distinguish between models with one or multiple epochs of reionization; and, although they suggest the possibility of an extended reionization epoch, the WMAP measures alone do not tightly constrain that possibility (Dunkley et al. 2008).

Much of the IGM in the nearby Universe is highly ionized, with a hydrogen neutral fraction $x_{\rm H~I} = N_{\rm H~I}/N_{\rm H~II} \sim 10^{-5}$ (Fan et al. 2006). A sensitive measure of the neutral hydrogen is to examine quasar spectra for the saturated trough shortward of Ly α caused by even a modest amount of neutral IGM gas, i.e., the classic Gunn-Peterson effect (Gunn & Peterson 1965). Somewhat in contrast to initial hints from the first few $z \sim 6$ quasars examined, data from ~ 20 now-studied high-redshift QSO sightlines, primarily from objects discovered in the Sloan Digital Sky Survey (SDSS; York et al. 2000), suggest that the reionization of H I likely happened before $z \sim 6$ (Fan et al. 2006). The H I Gunn-Peterson trough is evident in some $z \sim 6.3$ quasars (Becker et al. 2001; Fan et al. 2006), suggesting at least that the

ionization of hydrogen is patchy and may be rapidly evolving in the z>6 regime. However, there is marked sightline variance in the ensemble of quasar H I Gunn-Peterson measurements and their interpretations (e.g. White et al. 2003; Fan et al. 2006; Totani et al. 2006; Bolton & Haenelt 2007; Becker et al. 2007). Moreover, some high-redshift galaxy studies also tend to favor higher redshifts for H I reionization (e.g. Hu et al. 2002; Rhoads et al. 2004), as galaxies with strong (and inferentially, largely unabsorbed) H I Ly α emission are seen out to (at least) $z \sim 7$ (e.g. Iye et al. 2006).

Although hydrogen dominates both the number and mass fraction of baryons, helium is the most abundant absorber in much of the IGM accessible to current study. The He II reionization epoch is likely delayed versus that of H I because hard-ionizing sources such as AGN had to form to produce the higher energy photons needed (e.g. Wyithe & Loeb 2003). Even under the hard photoionizing conditions at $z \sim 2-4$, He II outnumbers H I by a factor of $\eta \sim 50\text{-}100$ (Fechner et al. 2006), and has a higher opacity by $\eta/4 > 10$. The He II Ly α transition is thus the more sensitive, higher opacity, empirical probe of much of the highly ionized IGM—as compared to H I which over most of sampled redshift space (between the H I Ly α forest lines) is extremely sparse. He II studies allow cosmological inferences about the epoch(s) of reionization, the intensity and spectrum of the ionizing background radiation, and measures of the cosmic baryon density in the IGM. However, He II Ly α absorption occurs in the far UV (304Å restframe), only observable from space in a rare fraction of high redshift quasars which lie by chance along clean lines of sight with little foreground absorption.

Jakobsen et al.'s pioneering work (Jakobsen et al. 1994) with the Hubble Space Telescope (hereafter, HST) provided the first detection of a He II Gunn-Peterson trough, in Q0302-003 (z = 3.29). Yet even following a further decade of effort, only four quasar sightlines suitable for He II Gunn-Peterson studies had been confirmed—though each was subjected to intensive UV spectral campaigns from HST, HUT, and/or FUSE. In redshift order these objects are: HS 1700+64 at z=2.72 (Davidsen et al. 1996; Fechner et al. 2006), HE 2347-4342 at z=2.88 (Reimers et al. 1997; Kriss et al. 2001; Smette et al. 2002; Zheng et al. 2004a; Shull et al. 2004), PKS 1935-692 at z = 3.18 (Anderson et al. 1999), and Q0302-003 at z = 3.29 (Jakobsen et al. 1994; Hogan et al. 1997; Heap et al. 2000). Broadly, the various intensive UV spectroscopic studies of these four quasars indicate that the IGM He II optical depth increases markedly from $\tau \sim 1$ near z = 2.5 to $\tau > 4$ at z = 3.3, and are also consistent with theoretical notions (Haardt & Madau 1996), and other indirect evidence (Songalia & Cowie 1996; Theuns et al. 2002), that helium reionization likely occurred near $z \sim 3$ (delayed vs. that of hydrogen at z > 6). These intensive follow-up studies have also provided a handful of empirical measures of the flux in the ionizing background radiation at $z \sim 3$ and the baryon density ($\Omega_q \sim 0.01$) in the IGM (e.g. Hogan et al. 1997; Zheng et al. 2004a; Tittley & Meiksin 2007). A predicted signature of the He II reionization epoch is a damping absorption profile redward of He II (Miralda-Escude 1998; Madau & Rees 2000); this feature was unseen in these four intensively studied cases at z < 3.3, but perhaps merely because they are at too low redshift (when He II ionization was well underway).

From later HST ultraviolet follow-up of selected optically bright high-redshift quasars, Reimers et al. (2005) identified QSO 1157+3143 (at z=3.0) as another He II quasar, and our group added three more clean quasar sightlines that extend helium IGM studies to the highest redshifts heretofore sampled (Zheng et al. 2004b). From an HST SNAP survey we first confirmed SDSS 2346-0016 (z = 3.5), SDSS 1711+6052 (z = 3.8), and SDSS 1614+4859 (z=3.8) as excellent new clean sightlines for helium IGM studies; our 6% selection efficiency, though modest, was among the highest then obtained. Moreover, our lengthy follow-up with the Advanced Camera for Surveys, Solar Blind Channel (ACS SBC) prism (taken after the failure of the Space Telescope Imaging Spectrograph [STIS]) for two of these, SDSS 2346-0016 and SDSS 1711+6052, shows an especially intriguing result: the z=3.8 case shows a surprisingly prominent absorption profile redward of the He II break location (Zheng et al. 2008) that is not seen in the z = 3.5 case. The profile in SDSS 1711+6052 is stronger and wider than commonly expected for the damped profile signature of the IGM, so in that paper we also consider additional explanations including absorption in a high-redshift intense starforming region. Whatever the explanation, the strength of this surprising feature demands further scrutiny in future high-quality UV spectra toward SDSS 1711+6052, as well as other comparably high-redshift He II quasar sightlines.

Motivated by the previous small sample size that limits confident global conclusions, and the potentially intriguing results at higher redshifts (e.g., Zheng et al. 2008), here we detail our successful efforts to markedly increase the number of new quasar sightlines suitable for the study of He II, across a broad redshift range. Starting from the very large sample of 7800 SDSS quasars at suitable redshift, we use the Galaxy Evolution Explorer (GALEX) archive to then cull to a new catalog of 200 higher-confidence far-UV detections of quasars at z > 2.78. An additional 112 quasar sightlines likely clean to high redshift are also similarly identified from cross-correlation of GALEX with other (non-SDSS) quasars. Our catalogs of likely far-UV-bright (restframe) quasars, presented in section 2, provide appropriate lists from which to draw for follow-up observations.

In section 3 we present reconnaissance UV observations with the *HST* ACS prism of 24 SDSS/*GALEX* candidate far-UV-bright quasars. Among these, we confirm 12 as bright in the far UV, with at least 9 evidently having flux all the way down to (very near) the He II break.

As we discuss in section 4, our SDSS/GALEX selection approach is thus found to be an order of magnitude more efficient than previous He II quasar searches, and herein we

more than double the number of clean sightlines spectroscopically confirmed as suitable for helium IGM studies. Moreover, our reconnaissance HST UV prism spectra suggest diversity, further confirming the need to obtain a large sample of independent quasar sightlines over a broad redshift range to understand cosmological variance and/or possible individual-object peculiarity.

2. SDSS/GALEX Selection and Catalogs of Far-UV-Bright Quasars

In order to identify a large new sample of clean sightlines to high redshift, we cross-correlate the very large SDSS quasar sample with the GALEX catalog of UV sources. SDSS is fundamental to the process, with its optical multicolor photometry and multi-object spectroscopy efficiently identifying a very large number of quasars out to high redshifts (Richards et al. 2002). The broadband GALEX catalog observations efficiently confirm which quasars are likely to have flux well into the far UV (restframe).

2.1. SDSS Quasar and GALEX Input Catalogs

The SDSS provides an optical digital imaging and spectroscopic data bank of a region approaching $\sim 10^4~\rm deg^2$ of sky, primarily centered on the north Galactic polar cap. Imaging and spectroscopic data are obtained by a special purpose 2.5m telescope, at Apache Point Observatory, New Mexico, equipped with a large-format mosaic camera that can image of order $10^2~\rm deg^2$ per night in 5 filters (u,g,r,i,z), along with a multifiber spectrograph that obtains 640 spectra, simultaneously, within a 7 deg² field. The imaging database is used to select objects for the SDSS spectroscopic survey, which includes spectrophotometry $(\lambda/\Delta\lambda \sim 1800)$ covering 3800-9200Å for 10^6 galaxies, 10^5 quasars, and 10^5 stars. Technical details on SDSS hardware and software, and astrometric, photometric, and spectral data may be found in a variety of papers: e.g., Fukugita et al. (1996), Gunn et al. (1998), Lupton et al. (1999), York et al. (2000), Hogg et al. (2001), Stoughton et al. (2002), Smith et al. (2002), Pier et al. (2003), Ivezić et al. (2004), and Gunn et al. (2006). A description of the most recent SDSS public data release (Data Release 6; hereafter, DR6) is given by Adelman-McCarthy et al. (2008).

The 5 SDSS optical filters plus multiobject spectra efficiently select quasars out to high redshifts. Here we focus on quasars from the SDSS catalog with redshift z > 2.78, for which the He II Ly α line at 304Å would then be observed at >1150Å. Observations in this wavelength regime must, of course, take place in space, and are thus currently limited

mainly to HST, although some fundamental observations of the brightest objects have been possible with FUSE (e.g. Kriss et al. 2001; Shull et al. 2004; Zheng et al. 2004a), and HUT (Davidsen et al. 1996) as well. Our specific choice of z > 2.78 here is motivated, in part, by the upcoming HST Service Mission 4; a refurbished STIS might be anticipated to be useful down to ~ 1150 Å, and the Cosmic Origins Spectrograph (COS) may even still have rather good response at this wavelength.

In the 5700 \deg^2 of sky with spectroscopic coverage in SDSS Data Release 5 (DR5), there are >77,000 spectroscopically confirmed quasars (Schneider et al. 2007), among which are nearly 6600 at z > 2.78 (e.g., see Figure 1). We include all such high-redshift confirmed DR5 quasars in our cross-correlation with GALEX. In addition, there are another 2300 SDSS candidate quasars potentially in this redshift regime in the further spectroscopic coverage of SDSS DR6. There is no officially vetted DR6 quasar catalog, so our search for the latter used the SDSS DR6 CasJobs table QSOConcordanceAll, which contains most of the likely quasar candidates. Given the likely contamination (usually by real quasars at incorrect redshifts) of this latter, not-yet-vetted set, we examined these additional DR6 spectra to exclude non-quasars and verify redshifts before matching to the GALEX catalogs. Our starting SDSS catalog thereby includes about 7800 spectroscopically confirmed SDSS quasars at z > 2.78.

However, identifying the small fraction of rare sightlines suitable in practice for He II studies demands UV observations as well. In order to be useful in constraining He II reionization and absorbers, the observed quasar spectra must have detectable flux down to the He II Ly α break, 304Å. Unfortunately, the UV fluxes of high-redshift objects are attenuated by accumulated absorption in numerous intervening HI Ly α lines (the Lyman Valley; Møller & Jakobsen 1990). Also, H I absorption from intervening Lyman-limit systems often severely cuts flux below 912Å(1 + z_{abs}). Only a few percent of random quasar sightlines to such high redshift are anticipated to be clear of this UV-obscuring neutral hydrogen (e.g., Møller & Jakobsen 1990; Reimers et al. 2005).

Hence, we cull through the 7800 SDSS z>2.78 optical quasars to find those most likely to be clean sightlines to high redshift, by cross-correlation with the GALEX catalogs. GALEX is performing a large-scale UV broadband imaging survey (Martin et al. 2005) in both the FUV (\sim 1350-1750Å) and NUV (\sim 1750-2800Å) bands. There are three surveys: the all-sky survey (AIS) extends to $m_{\rm AB} \sim 21$, and the much smaller area medium and deep surveys (MIS and DIS) extend to $m_{\rm AB} \sim 23$ and $m_{\rm AB} \sim 25$, respectively. The GALEX GR2 and GR3 catalogs (henceforth GR2/GR3) are complementary data sets processed with the same pipeline and constituting one catalog (Morrissey et al. 2007). GR2/GR3 covers \sim 13,500 deg² of sky, but the GALEX sky coverage does not contain all the SDSS DR5/DR6 spectroscopic sky coverage. Among the 7800 SDSS z>2.78 quasars discussed above, GALEX

GR2/GR3 provides UV imaging coverage for 4704 (3913 from the vetted DR5 catalog, and 791 more from DR6 only). It is these 4704 SDSS quasars that are actually matched to GALEX GR2/GR3 UV catalogs, and considered further in the next subsection. Although the broadband GALEX observations do not provide sufficient information to conclusively confirm far-UV flux all the way down to He II, they at least may confirm which of our quasars have flux well into the restframe far UV, i.e., to UV wavelengths where most random quasar sightlines are obscured by intervening clouds.

2.2. SDSS/GALEX Cross-Correlation

A key parameter in the cross-correlation of catalogs is the maximum SDSS/GALEXpositional match radius. Of course this depends on the FWHM of FUV and NUV GALEX point-spread functions, as noted below. But this also depends in part on the astrometric accuracy of the surveys. Since the SDSS astrometric accuracy is better than 0.1" (Pier et al. 2003), the modest astrometric limiting factor is GALEX, with accuracy of about 0.5" rms (Morrissey et al. 2007). (A match radius based on only this formal error would be an underestimate, since, unsurprisingly, the non-gaussian separation distribution has a long tail.) The optimal match radius also depends on the surface density of the objects of interest; we are somewhat inclusive in our choice because there are comparatively few He II candidates. This is weighed against the background rate of GALEX sources contributing as false matches. Because our targets are found on a unique mixture of AIS, MIS, and DIS images, we preferred a direct measure of the best match radius for our particular application. To characterize the background rate of happenstance positional coincidences, we performed matching between mock SDSS quasar catalogs and the GALEX catalog, by randomly shifting from our actual SDSS quasar positions. These shifts were in various mixtures of RA and Dec, and of a few arcminutes each. This is large enough to be well outside the original match radius, but generally to remain on the same GALEX 1.25°-field-of-view tile image as the true search (and hence sampling to a very similar *GALEX* depth).

We initially considered a match radius extending out to r < 6'' (in both actual, and in mock Monte Carlo, catalog matches); this starting radius was chosen because the GR2/GR3 spatial resolution is about 5.3" FWHM in the NUV (Morrissey et al. 2007). We verified that the spurious matches in the Monte Carlo shifts were uniform in r^2 , as should be the case. This uniform background is shown in Figure 2 overplotted on our actual cross-correlation of SDSS/GALEX catalogs. From our mock-catalog Monte Carlo shifting considerations, we determined that a cut at about r < 3'' match radius might be effective in avoiding most spurious matches; at match radius r < 3'', our Monte Carlos suggest that about r < 2%

of cases are likely real SDSS quasar/GALEX UV source associations, with 30% spurious matches. Very few real associations are outside of this match radius, although UV sources that are too faint to be extracted into the GALEX catalog will of course go unnoticed. (For comparison, we estimate that $\sim 20\%$ of true matches found within 3" would be outside of a 2" radius.)

Morrissey et al. (2007), in their review of GALEX performance, recommend cross-correlating GALEX and catalogs of higher astrometric accuracy with a maximum search radius of 2", for many purposes. We choose the slightly more generous r < 3" limit for several reasons. First, Morrissey et al. (2007) considered mainly UV-bright sources, while we are concerned with many sources near the UV detection limits; our own analysis and that of others (including Morrissey et al. 2007) reveal, unsurprisingly, that higher S/N detections tend to have higher astrometric accuracy. Second, we have a number of quasars detected in FUV only, and the FUV astrometric precision is worse than that of the NUV (Morrissey et al. 2007). Third, our comparison with HST reconnaissance observations of some of the objects on our list (see section 3) ultimately empirically confirms that 3" is an appropriate balance between getting most true matches and excluding most spurious ones. Fourth, a number of other SDSS/GALEX studies (e.g., Agüeros et al. 2005; Trammell et al. 2007) also prefer allowing offsets out to about 3".

Among the 4704 SDSS DR5/DR6 z > 2.78 quasars within the GALEX GR2/GR3 area, we find 419 unique matches within a match radius of r < 6". (We preferred closer matches in the cases where more than one UV source was within the search radius of the SDSS optical object.) Among these 419, there are 212 within our ultimately preferred r < 3" match radius.

Finally, we inspected both the SDSS and GALEX images for the positionally preferred 212 cases, for any obvious problems. No further objects were removed based on SDSS image concerns, but several cases were flagged as having very near optical neighbors. These projected neighbors may lead to complications in at least two ways for helium IGM studies: first, if the projected neighbor is an intervening galaxy, then the quasar UV spectroscopic sightline might be impacted by low-redshift H I or other absorption from the galaxy (or group/cluster in which the projected neighbor galaxy resides); second, the neighboring optical object might actually be the GALEX source, rather than the quasar. We also inspected the GALEX images, both NUV and FUV, looking for catalog matches where the UV object appeared to be an artifact. (Note the GR2/GR3 catalogs have artifact flags for each object which we consulted as well.) After removing GALEX artifact matches, and those too close to GALEX tile edges or other artifacts to be certain of the identification, we were left with the 200 objects that constitute our final catalog of higher confidence SDSS/GALEX quasars

at z > 2.78.

All of the previously confirmed He II quasars in our SDSS position and redshift footprints are recovered in our higher confidence catalog in a blind fashion. These include the quasars: Q0302-003 (z=3.29; Jakobsen et al. 1994), SDSS J2346-0016 (z=3.51; Zheng et al. 2004b), SDSS J1614+4859 (z=3.80; Zheng et al. 2005), and SDSS J1711+6052 (z=3.83; Zheng et al. 2008); see magenta stars in Figure 1. In addition, OQ172 (z=3.54; Lyons et al. 1992, 1994, 1995; Jakobsen et al. 1993), a very bright quasar considered and rejected as a He II candidate in very early HST UV studies (with a break just redward of He II Ly α) is also recovered in our catalog (see red star symbol at z=3.54 in Figure 1), further reassuring that we are not missing many potentially interesting objects.

2.3. Catalog of Far-UV-Bright SDSS/GALEX Quasars

The 200 SDSS quasars at z > 2.78, associated at higher ($\sim 70\%$) confidence with GALEX UV sources (3" match radius) are cataloged in Table 1. Selected basic data are also displayed in Figures 1 and 3 (see medium, filled black circles depicting the 200 quasars).

In Table 1, the catalog columns for these candidate far-UV-bright (restframe) quasars are as follows. Columns 1-5—Names, positions (RA, dec; J2000), redshifts, and magnitudes are all from SDSS. The redshift is from the automated pipeline, but we verified it to be reasonably accurate in each case, via our by-eye examinations of the spectra. Columns 6-7—The GALEX catalog provides fluxes in μ Jy, which we have converted to erg s⁻¹ cm⁻² Å⁻¹ using the effective wavelengths of the GALEX broadband filters: 2267Å for NUV, and 1516Å for FUV. Column 8—Inspection flag. This is a 4-bit integer flag, reflecting our by-eye inspection SDSS/GALEX images and SDSS spectra. We inspected the SDSS images, and if there was a galaxy or possible galaxy nearby in projection (typically within 10"), or a very near blue object (typically within 5"), this flag gets a value of 1. A value of 2 indicates that we saw a probable Lyman-limit system (LLS) or damped hydrogen Ly α absorber (DLA) in the optical SDSS spectrum. A value of 4 is given to those objects that are broad absorption line quasars (BALQSOs; defined herein as having broad C IV absorption in excess of 2000 km s⁻¹), and a value of 8 is given to those objects that are borderline on our BALQSO criterion. These flags are additive, and hence a flag of 6 here would mean a BALQSO that also has a LLS or DLA. Column 9—HST observation flag. The observation flag is 0 if the object has not been observed with HST, 1 if it has been observed with FUV (to near 304Å rest) spectroscopy through HST cycle 16, and 2 if it has been observed less conclusively, i.e., NUV spectroscopy, UV imaging, or pre-COSTAR observation.

2.4. Catalog of Other Far-UV-Bright GALEX Quasars

In addition to the SDSS quasars, we similarly matched the quasar catalog of Véron-Cetty & Véron (2006) to GALEXGR2/GR3 as well. There are 1144 z > 2.78 quasars in Véron-Cetty & Véron (2006) that are not in SDSS DR6, of which 705 are in the GALEX footprint. We performed the same match radius determination described above on this non-SDSS quasar compilation, and found a match radius of 3.5" was a better compromise in this case, perhaps reflecting the more heterogeneous astrometric heritage of these quasars. Within this radius, there were 112 matches (84 \pm 1% likely true matches) to GALEX GR2/GR3 sources; hereafter, we refer to these as the VCV/GALEX quasars. (One additional match was discarded since it also matched a low-redshift SDSS quasar; the SDSS redshift was verified to be correct.) Although accurate optical magnitudes on a common system are not uniformly available for these VCV/GALEX quasars, they may be slightly brighter in the optical than the SDSS sample, and this may contribute some to the higher match rate to GALEX. However, given the steep increase in intervening obscuration with redshift, it seems more plausible that the higher match rate is mainly a redshift effect. As may be seen in Figure 4, the redshift distribution of the VCV/GALEX quasars favors systematically lower-redshifts than the SDSS quasar sample, which generally extends to quite high-redshift (e.g., Anderson et al. 2001); for example, only about 1/4 of the VCV/GALEX matches are at z > 3.05 compared to about 1/2 of the SDSS/GALEX matches. No inspection flag was readily feasible for these additional quasars, given the difficulty of obtaining uniform optical images and spectra for this heterogeneous sample. Our catalog of VCV/GALEX far-UV-bright (restframe) quasars is provided in Table 2.

In Table 2, the catalog columns for these far-UV-bright (restframe) quasar candidates are as follows. Columns 1-5—Names, positions (RA, dec; J2000), redshifts, and magnitudes are all from Véron-Cetty & Véron (2006) and the specific references cited therein. The optical magnitude provided is a V magnitude unless otherwise marked as: photographic (*), blue (B), red (R), infrared (I J K), or photographic O- or J- plates (O). Columns 6-7—The GALEX catalog provides fluxes in μ Jy, which we have converted to erg s⁻¹ cm⁻² Å⁻¹ using the effective wavelengths of the GALEX broadband filters: 2267Å for NUV, and 1516Å for FUV. Column 8—HST observation flag. The observation flag is 0 if the object has not been observed with HST, 1 if it has been observed with FUV (to near 304Å rest) spectroscopy through HST cycle 16, and 2 if it has been observed less conclusively, i.e., NUV spectroscopy, UV imaging, or pre-COSTAR observation.

Again, reassuringly, we recover in a blind fashion both additional previously confirmed He II quasars that might be anticipated to be among our VCV/GALEX finds, PKS 1935-692 (z=3.18) and HE 2347-4342 (z=2.88) (see magenta stars in Figure 3). In addition, UM670

(z=3.16; Jakobsen et al. 1993; Lyons et al. 1994), another very bright quasar considered and rejected as a He II candidate in very early HST UV studies (with a break just redward of He II Ly α) is also recovered in our catalog (see red star symbol in Figure 3). Finally, note that there are only two further venerable He II quasars (see large green circles in Figure 3, lacking a central black point) to account for that do not appear in our catalogs. But these two are absent from our catalogs for fully anticipated reasons: HS 1157+3143 (Reimers et al. 2005) is not within the GALEX GR2/GR3 footprint, while HS 1700+64 (Davidsen et al. 1996) falls just below our catalog redshift cut.

The 200 SDSS and 112 other z>2.78 quasars cataloged in this and the previous subsections represent significant resource lists for far-UV (restframe) studies of quasars. Our UV-bright quasars may find applications to a range of studies from the study of far-UV SEDs, emission lines, and BALs, to study of low-redshift hydrogen absorbers, to our interest in He II. In the next section we focus on preliminary reconnaissance follow-up observations from HST of selected SDSS/GALEX quasars, relevant to our primary aim of identifying a large new sample of independent, clean sightlines potentially suitable for helium IGM studies.

3. HST/ACS-Prism Confirmation of a High Yield of Far-UV-Bright Quasars

3.1. Reconnaissance HST UV Spectroscopy

In HST cycles 15 and 16 (GO programs 10907 and 11215), we conducted programs of brief reconnaissance UV spectra of some of our SDSS/GALEX quasars; we have observed 24 of our SDSS/GALEX candidate quasars with brief UV ACS/SBC prism spectra to verify end-to-end their potential suitability for future detailed He II studies. Our HST target list was originally based on the then-available GALEX GR1 catalogs, supplemented later by expansions to GALEX GR2/GR3 (as well as continuing expansions in the SDSS quasar catalogs). Three of the 24 HST targets appeared as UV sources in the GALEX GR1 catalog, but not (at least within a 6" offset) in the later GR2/GR3 catalog. However, the bulk we observed with HST are indeed in GALEX GR2/GR3 catalogs, also providing an end-to-end test of our SDSS/GALEX selection approach discussed in section 2. About half of our HST targets had SDSS/GALEX positional offsets (at least in the GR2/GR3 catalog) in the range r < 3", and about half beyond r > 3".

The reconnaissance UV spectra (plus accompanying direct UV images described below) encompass 2 *HST* orbits each, with a total of 6 individual prism exposures for each object; individual exposures are about 600-800s each, with typical total exposure times of about 3-5 ksec for the coadded spectrum for each quasar. The prism PR130L was used to limit

complications (e.g., markedly enhanced backgrounds) due to geocoronal Ly α , and effectively covers the wavelength range of about 1250-1750Å. (In some cases we cautiously use data 10 or 20Å blueward, to help constrain the behavior of the lower-redshift objects. Although the sensitivity of PR130L falls quickly below 1250Å, it is not zero.) Our HST observations and reductions also involve, for each object, four \sim 100s direct UV image exposures with ACS/SBC using the F150LP filter, needed to establish the prism spectra wavelength zero points.

A total of 12 of the targeted 24 quasars are verified with HST to have detectable far-UV (restframe) flux in the ACS PR130L wavelength regime. While not all of those are suitable for He II IGM studies, the majority are, and our HST reconnaissance results confirm the very high yield of far-UV-bright quasars obtainable from SDSS/GALEX cross-correlations for r < 3'' offsets. Only two of the r < 3'' cases observed in our HST reconnaissance lack a UV flux detection in our prism data. Moreover, one of those two is actually also excluded from our current catalog of 200 higher confidence far-UV bright quasars discussed in section 2; it was among the r < 3'' positional matches, but excluded in section 2 at the final culling stage when examining GALEX images, as a possible GALEX artifact. (This exclusion was based on GR2/GR3 data not available at the time of HST observation.)

The 12 far-UV-bright confirmations from our HST prism reconnaissance are listed in Table 3. Tabulated are the following columns. Columns 1-4—Names, positions (RA, dec; J2000), and redshifts are all from SDSS. The redshifts are from the automated pipeline, but we verified them to be reasonably accurate in our by-eye examination (only one case, 0808+4550, required a redshift adjustment, by 0.05). Columns 5-6—The GALEX catalog provides fluxes in μJ_v , which we have converted to erg s⁻¹ cm⁻² Å⁻¹ using the effective wavelengths of the GALEX broadband filters: 2267Å for NUV, and 1516Å for FUV. The errors quoted are those given by the GALEX catalog. Columns 7-8—Exposure times and date the target was observed with HST ACS. The exposure times indicate how much data was used to produce each final coadded spectrum. In cases where we discarded some particularly noisy or misaligned exposures, this differs a little from the actual total exposure time. Column 9—Indicates whether or not there is a sharp break at a wavelength consistent with that expected for He II Ly α . Quasars identified in the table as likely having a break at He II, conservatively must show a break of comparable width to (or a little wider than, as expected for a proximity feature) the prism instrumental resolution. (Other objects listed as uncertain in Table 2 may nonetheless also still be of potential interest for future He II studies.) Note that no objects have obvious significant flux that extends blueward of the expected break location, although this is not well constrained in the lower-redshift cases.

3.2. Basic *HST* UV Prism Spectral Reductions

For the 12 cases with ACS/HST prism detections, we reduced the ACS 2-D spectra with the aXe software, version 1.6 (Kümmel et al. 2006). We consulted both SExtractor and IRAF tasks applied to the direct F150LP images to determine the positional information input needed for aXe. The spectrum from each individual 600s-800s exposure was extracted separately, with local background subtraction. In almost every case, our targets were the only objects evident in the UV HST exposures. For each quasar we coadded the multiple individual 600s-800s extracted spectra. This was complicated by the lack of a common wavelength scale, which we accounted for by fitting each spectrum with a high-order cubic spline (with knots determined by the first exposure's wavelength scale). These fits matched the original data to $\lesssim 0.1$ -1%, and thus were a negligible source of error. We examined each individual exposure's spectrum, and discarded those that were vastly more noisy than the average. These fitted individual exposure spectra, now with a common wavelength scale, were then averaged for each quasar. The discarded exposures were about $\sim 10\%$ of the total observation time, and no more than $\sim 25\%$ for any given quasar.

Relative fluxes in these initial prism reductions should be reasonably good, but possible systematic errors in absolute spectrophotometry zero-points are a residual concern and under continuing study (though they do not impact any conclusions herein). For example, errors in determining the target's position in the F150LP images would lead to systematically lower fluxes since the extraction trace would not be exactly along the spectrum. Another factor that affects flux measurements is the weighting used during the extraction from the 2-D spectrum. Here, we have chosen to use optimal weighting (Horne 1986) as implemented by aXe, which uses lower weights for pixels farther from the spectrum's trace (on the axis perpendicular to dispersion) to improve S/N; such optimal weighting may tend to also underestimate the flux zeropoints (though alternate weightings at least give very similar relative fluxes). Finally, there appears to be some possible systematic underestimate of the spectral flux compared to the GALEX broadband data.

The extracted, coadded spectra of the 12 far-UV-bright quasars confirmed from HST are presented in Figure 5a and 5b. The vertical dotted line shows the wavelength of expected IGM He II absorption for the given quasar redshift. The absolute flux calibration is uncertain, as noted above, but the relative flux calibration is more secure. The width of the bins is about half of the instrumental resolution at the given wavelength (for PR130L, R ranges from about 350 at 1250Å to about 60 at 1670Å).

4. Discussion: A High Yield of New Sightlines for Helium Studies

The ACS prism data shown in Figure 5 confirm that our catalogs presented in section 2 are successful in including most real matches and excluding most false matches. Among the 24 SDSS/GALEX quasars with reconnaissance HST spectra, about half have SDSS/GALEX positional offsets in the range r > 3'', but none of those were confirmed as having significant far-UV (restframe) flux in the ACS prism data; this further confirms our choice to catalog only the higher confidence cases with r < 3'' in section 2. Among our 200 higher-confidence SDSS cases cataloged, we have observed 11 with ACS/prisms. Ten of the 11 such higher-confidence cases from our cycle 15-16 observations are confirmed as far-UV-bright (restframe) in our reconnaissance ACS spectra. In fact, the HST reconnaissance ACS prism observations were first initiated based on GALEX DR1 catalogs, and we also have two additional quasars (SDSS 1009+3917 and SDSS 1137+6237) that appear as GALEX sources at r < 3'' in GALEX DR1, but not in GR2/GR3; both of these quasars are also confirmed in our HST/prism spectra to be bright in the far UV.

Of the total of 12 cases definitively verified as far-UV-bright from HST prism spectra, at least 9 show surviving flux all the way down to very near the wavelength expected for IGM He II Ly α , and are potentially suitable for additional helium IGM UV-spectroscopy studies. These are SDSS 0139-0847 (z=3.13), SDSS 0941+5607 (z=3.79), SDSS 1006+3705 (z=3.20), SDSS 1007+4723 (z=3.41), SDSS 1009+3917 (z=3.83), SDSS 1137+6237 (z=3.78), SDSS 1442+0920 (z=3.53), SDSS 2200+0008 (z=3.13), and SDSS 2251-0857 (z=3.12). One case, SDSS 0808+4550 (z=3.15) appears strongly absorbed with a sharp break ~ 65 Å redward of He II; perhaps this is due to a strong low-redshift hydrogen absorber at z=0.45. Somewhat more ambiguous are SDSS 0056-0941 (z=3.25) and our highest-redshift case, SDSS 1319+5202 (z=3.90), both of which appear to have more gradual absorption starting ~ 60 Å redward of He II. None of our spectra show highly significant flux blueward of the He II break, consistent with the IGM helium having a non-negligible neutral or singly-ionized fraction in the broad redshift range probed. However, the spectra are of very low S/N, and in the lower-redshift cases there are very few data below the break.

Therefore, our approximate efficiency in identifying far-UV-bright quasars is of order 50% (raw success rate among HST-observed cases) up to 90% (using the criteria of the higher-confidence catalogs of section 2). Our efficiency in identifying new He II quasar sightlines is $\sim 35\%$ (raw success rate among HST-observed cases) to $\sim 65\%$ (using the higher-confidence criteria of the catalogs presented in section 2). These efficiencies are also consistent with our spurious superposition estimates of section 2. But note that even among the higher confidence subset, reconnaissance HST observations to confirm flux all the way down to He II are desired before undertaking lengthy follow-up UV spectral observations. In any

case, our efficiency is confirmed to be an order of magnitude better than previous searches for He II quasars, at $\sim 35-65\%$.

Some further caution is also appropriate in attributing any precise efficiency expectation to the other quasars cataloged in section 2, but not yet observed with HST. The quasars chosen for initial HST reconnaissance spectra are not a random sample for several reasons: (1) On average, the UV-brighter SDSS objects (as indicated by GALEX) were preferentially selected (see Figure 3) for spectroscopic observation with ACS, and thus constitute a potentially biased subset of our Table 1 catalog. (2) Competing somewhat with the last bias is the need to extend He II studies to higher redshifts, especially to confirm, e.g., the damped red profile expected at the reionization epoch; we thus often chose for HST prism reconnaissance the UV-brightest object in a given higher-redshift bin, in preference over adding many more UV-brightest cases at $z \sim 3$, where there are several very well-studied quasar sightlines in the literature (see Figure 3, large green circles). (3) We also excluded from HST observations quasars that were strongly absorbed in their SDSS optical spectra. While our HST data thus demonstrate an unprecedentedly high efficiency for the UV-brighter (and optically cleanest) objects, they do not directly confirm the fraction of fainter GALEX objects in our catalog that are true SDSS/GALEX matches, nor assess the match efficiency of heavily (optically) absorbed cases such as BALQSOs. That there are two quasars confirmed in our reconnaissance HST observations (SDSS 1010+3917 and SDSS 1137+6237) that appear in the GR1 catalog, but not in GR2/GR3 GALEX catalogs, suggests at least modest incompleteness as one reaches the GALEX UV depth limits (though completeness is not a consideration for our primary He II science).

On the other hand, the UV-brightest of our new spectroscopically confirmed He II quasars, such as SDSS 1006+3705 at z=3.20, are comparable to the best of the venerable well-studied He II quasars. The far-UV (restframe) flux of this latter quasar is of order 10^{-16} erg s⁻¹ cm⁻² Å⁻¹, similar to Q0302-003, for example. There are a number of other such likely cases in our catalogs presented in section 2, though many of the very UV-brightest cases are in the already reasonably well-studied z<3.1 regime (Figure 3); future studies may benefit from exploring the UV-brightest quasars in a given redshift regime. But even the bulk of our cataloged likely SDSS/GALEX matches are well within expectations for future detailed observations with HST. For example, the pre-flight COS estimated time calculator indicates that 1-orbit observations of objects with UV fluxes down to $\sim 5 \cdot 10^{-18}$ erg s⁻¹ cm⁻² Å⁻¹ would yield spectra of sufficient quality to sample a proximity zone near a He II Ly α break (S/N \sim 5 for 3 bins across a typical 20Å wide, $\tau \sim 1$ proximity zone, for objects in most of our redshift range). The great bulk—about 97%—of the objects in Tables 1 and 2 satisfy such criteria.

Comparison of Figures 1 and 3 also allows one to infer another result, perhaps not widely recognized. Most historical UV searches for He II quasars emphasized searches mainly of the optically brightest quasars. While there is a correlation, these figures highlight that the optical is often not a good predictor of surviving quasar far-UV flux; many of the cases confirmed as far-UV bright in our *HST* reconnaissance are optically comparatively faint. The additional use of *GALEX* selection is essential to efficiently cull to the best new sightlines.

Our HST prism spectra are presented herein primarily to verify the utility of our SDSS/GALEX selection approach (with initial efficiency estimates), and of course to definitively verify at least 9 new clean He II quasar sightlines. However, the (admittedly modest S/N) individual spectra displayed in Figure 5 also already suggest some diversity in far-UV (restframe) spectral character worthy of further study. The 9 aforementioned quasars/sightlines appear fairly clean and not too dissimilar to earlier He II quasars. However, there are three cases (SDSS 0056-0941, 0808+4550, 1319+5202) that are strongly absorbed starting ~ 60 A redward of the He II break. It may be worth recalling that other optically bright quasars, such as UM670 and OQ172, considered but rejected in early HST He II searches, also appear to have redward breaks (Lyons et al. 1994, 1995; Jakobsen et al. 1993)]. And in our own HST confirmation there are at least two quasars (SDSS 1006+3705, 1442+0920) perhaps with unusually strong far-UV emission features. This diversity reinforces the utility of initial reconnaissance HST observations in planning for more detailed UV spectral follow-on observations. It also emphasizes the necessity of obtaining a large sample of independent He II quasar sightlines, spanning a broad redshift range, to allow adequate averaging over cosmic variance and/or individual-object pathology in helium studies. (Of course even if some or all of the redward-absorbed cases discussed herein are ultimately understood as unsuitable for IGM He II studies, they may still be potentially interesting for studies of low-redshift hydrogen absorbers, for example).

It may also be of interest to broadly compare our ensemble prism spectra here with the ACS prism spectrum (same instrumental setup, but much longer exposure and better S/N) of the intriguing He II quasar SDSS J1711+6052 detailed in Zheng et al. (2008). In that paper, we discuss the possibility that the spectral character of SDSS 1711+6052 observed redward of the expected (1465 Å) He II break location might be associated with the red wing of He II Ly α emission, strongly absorbed by a very broad damped profile. That damped profile might arise from low-redshift hydrogen, or interestingly perhaps from a surprisingly dense (column density $\sim 10^{22}$ cm⁻²) helium Ly α absorption at high redshift, for example. An ensemble stack of the UV spectrum of seven of our new clear quasar sightlines at z < 3.5 (in the observed wavelength frame) is shown in Figure 6. This stacked ensemble spectrum is largely devoid of very strong features in the instrumental frame near 1400-1500Å, i.e., devoid of very strong features near the observed wavelength of the possibly damped profile seen in

SDSS 1711+6052. This stacked ensemble ACS spectrum then would seem to at least argue strongly that the possibly damped profile absorption feature discussed in Zheng et al. (2008) for SDSS J1711+6052 is unlikely merely some instrumental artifact of ACS prisms.

5. Summary and Concluding Remarks

We provide a catalog of 200 higher-confidence (\sim 70% secure) SDSS quasars at z>2.78 that are likely statistically associated with GALEX ultraviolet sources. We provide an additional set of 112 similar quasars, also z>2.78 but on average lower redshift, from consideration of the Véron-Cetty & Véron (2006) quasar compilation. Our catalogs herein comprise very large resource lists (two orders of magnitude larger than previous similarly dedicated efforts) of likely far-UV (restframe) bright quasars, potentially of interest for a range of studies from far-UV SED, emission line, and BALQSO spectral studies, to background probes of intervening clouds including H I at low-redshift, to our own primary interest in the He II Gunn-Peterson test.

We report reconnaissance UV spectral observations from HST of 24 SDSS/GALEX selected quasars, chosen to encompass a wide redshift range, finding that half are indeed far-UV bright. At least 9 new quasars are confirmed in our HST prism spectra as suitable new sightlines for He II Gunn-Peterson studies. The HST data also allow us to confirm the even higher efficiency of our refined selection approach, which generated the catalogs of section 2. In either case, our combined SDSS/GALEX/HST-reconnaissance selection efficiency is an order of magnitude better than previous similar He II quasar searches, and we herein more than double the number of spectroscopically confirmed He II quasars.

Our HST prism spectra show some diversity, reaffirming the need for UV reconnaissance spectral observations to confirm that UV flux extends all the way down to He II (even in cases detected in broadband from GALEX). The spectral diversity found also confirms the necessity of identifying multiple independent clean sightlines, covering a broad redshift range, to limit cosmological variance and individual-object pathology in seeking global understanding from helium IGM studies. An observed-frame ensemble stack of our HST reconnaissance spectra suggests that the strong absorption seen in SDSS1711+6052 by Zheng et al. (2008) redward of the He II break is unlikely to be an instrumental artifact.

To probe IGM He II in detail, including the epoch of He II reionization, requires a large enough sample of clean quasar sightlines, extending over a broad redshift range, in order to be limited by cosmic variance rather than individual peculiarities or a clumpy IGM. With such a large, broad-redshift sample, concerns of a possible systematic bias due to clear sightline selection may be addressable using the observed sightlines to calibrate large-scale numerical simulations of reionization (e.g., Wyithe et al. 2008). The range of redshift encompassed by our sample may also allow future observations to constrain percolation models of reionization, such as the one discussed by Paschos et al. (2007).

The empirical surprises at high redshift (Zheng et al. 2008), theoretical uncertainties in interpreting the past low redshift results (Meiksin 2008), and the broad goal of identifying the epoch of helium reionization through the anticipated redward damped He II profile signature, all argue strongly for the need to emphasize He II Gunn-Peterson studies beyond the $z\sim3$ regime of the bulk of the venerable past studies. Our catalogs of hundreds of far-UV-bright quasars, and even more directly our HST spectroscopic confirmations of at least 9 new He II quasars (along with several more from our earlier similar work), provide basic resource lists extending to such higher redshifts for future detailed (good S/N and spectral resolution) UV spectral science investigations of helium in the IGM.

Funding for the SDSS and SDSS-II has been provided by the Alfred P. Sloan Foundation, the Participating Institutions, the National Science Foundation, the U.S. Department of Energy, the National Aeronautics and Space Administration, the Japanese Monbukagakusho, the Max Planck Society, and the Higher Education Funding Council for England. The SDSS Web Site is http://www.sdss.org/.

The SDSS is managed by the Astrophysical Research Consortium for the Participating Institutions. The Participating Institutions are the American Museum of Natural History, Astrophysical Institute Potsdam, University of Basel, University of Cambridge, Case Western Reserve University, University of Chicago, Drexel University, Fermilab, the Institute for Advanced Study, the Japan Participation Group, Johns Hopkins University, the Joint Institute for Nuclear Astrophysics, the Kavli Institute for Particle Astrophysics and Cosmology, the Korean Scientist Group, the Chinese Academy of Sciences (LAMOST), Los Alamos National Laboratory, the Max-Planck-Institute for Astronomy (MPIA), the Max-Planck-Institute for Astrophysics (MPA), New Mexico State University, Ohio State University, University of Pittsburgh, University of Portsmouth, Princeton University, the United States Naval Observatory, and the University of Washington.

We gratefully acknowledge support from NASA/GALEX Guest Investigator grants NNG05GE12G and NNG06GD03G. Support for HST Program numbers 10132, 10907, and 11215 was provided by NASA through grants from the Space Telescope Science Institute, which is operated by the Association of Universities for Research in Astronomy, Incorporated, under NASA contract NAS5-26555.

REFERENCES

Adelman-McCarthy, J.K., et al. 2008, ApJS, 175, 297

Agüeros, M. A. et al. 2005, AJ, 130, 1022

Anderson, S. F., Hogan, C. J., & Williams, B. F. 1999, AJ, 117, 56

Anderson, S. F., et al. 2001, AJ, 122, 503.

Becker, R. H. et al. 2001, AJ, 122, 2850

Becker, G. D., Rauch, M., & Sargent, W. L. W. 2007, ApJ, 662, 72

Bolton, J.S., & Haehnelt, M.G. 2007, MNRAS, 374, 493

Davidsen, A. F., Kriss, G. A., & Zheng, W. 1996, Nature, 380, 47

Dunkley, J. et al. 2008, ApJS, in press (arXiv:0803.0586)

Fan, X., Carilli, C. L., & Keating, B. 2006, ARA&A, 44, 415

Fechner, C. et al. 2006, ApJ, 455, 91

Fukugita, M., Ichikawa, T. Gunn, J.E., Doi, M., Shimasaku, K., & Schneider, D.P. 1996, AJ, 111, 1748

Gunn, J. E. & Peterson, B. A. 1965, ApJ, 142, 1633

Gunn, J.E., et al. 1998, AJ, 116, 3040

Gunn, J.E., et al. 2006, AJ, 131, 2332

Haardt, F., & Madau, P. 1996, ApJ, 461, 20

Heap, S. R., Williger, G. M., Smette, A., Hubeny, I., Sahu, M. S., Jenkins, E. B., Tripp, T. M., Winkler, J. N. 2000 ApJ, 534, 69

Hogan, C. J., Anderson, S. F., & Rugers, M. H. 1997, AJ, 113, 1495

Hogg, D.W., Finkbeiner, D.P., Schlegel, D.J., & Gunn, J.E. 2001, AJ, 122, 2129

Horne, K. 1986, PASP, 98, 609

Hue, E. et al. 2002, ApJ, 568, L75

Ivezić, Ż., et al. 2004, AN, 325, 583

Iye, M. et al. 2006, Nature, 443 186

Jakobsen, P. et al. 1993, ApJ, 417, 528

Jakobsen, P., Boksenberg, A., Deharveng, J. M., Greenfield, P., Jedrzejewski, R., & Paresce, F. 1994, Nature, 370, 35

Kriss, G. et al. 2001, Science, 293, 1112

Kümmel, M., Larsen, S.S., & Walsh, J.R. 2006, in Hubble after the transition to two-gyro mode, ed. A. M. Koekemoer, P. Goudfrooij, & L. L. Dressel, (NASA/GFSC), 85

Lupton, R.H., Gunn, J.E., & Szalay, A. 1999, AJ, 118, 1406

Lyons, R. W., Beaver, E. A., Burbidge, E. M., Cohen, R. D., & Junkkarinen, V. T. 1992, BAAS, 24, 1136

Lyons, R. W., Cohen, R. D., Hamann, F. W., Junkkarinen, V. T., Beaver, E. A., & Burbidge, E. M. 1994, BAAS, 185, 1801

Lyons, R. W., Cohen, R. D., Junkkarinen, V. T., Burbidge, E. M., & Beaver, E. A. 1995, AJ, 110, 1544

Madau, P. & Rees, M.J. 2000, ApJ, 542, 69

Martin, D.C., et al. 2005, ApJL, 619, L1

Meiksin, A.A. 2007, Reviews of Modern Physics, submitted (arXiv:0711.3358).

Miralda-Escude, J. 1998, ApJ, 501, 15

Møller, P. & Jakobsen, P. 1990, A&A, 228, 299

Morrissey, P. et al. 2007, ApJS, 173, 682

Paschos, P., Norman, M. L., Bordner, J. O., & Harkness, R. 2007, arXiv:0711.1904

Pier, J. R., Munn, J. A., Hindsley, R. B., Hennessy, G. S., Kent, S. M., Lupton, R. H., & Ivezić, Ž. 2003, AJ, 125, 1559

Reimers, D., Kohler, S., Wisotzki, L., Groote, D., Rodriguez-Pascual, P., & Wamsteker, W. 1997, A&A, 327, 890

Reimers, D., Fechner, C., Hagen, H.-J., Jakobsen, P., Tytler, D., & Kirkman, D. 2005, A&A, 442, 63

Rhoads, J.E. et al. 2004, ApJ, 611, 59

Richards, G. T. et al. 2002, AJ, 123, 2945

Schneider, D. P. 2007, AJ, 134, 102

Shull, J. M., Tumlinson, J., Giroux, M. L., Kriss, G. A., & Reimers, D. 2004, ApJ, 600, 570

Smette, A., Heap, S. R., Williger, G. M., Tripp, T. M., Jenkins, E. B., & Songaila, A. 2002, ApJ, 564, 542

Smith, J.A., et al. 2002, AJ, 123, 2121

Songaila, A., & Cowie, L.L. 1996, AJ, 112, 335

Stoughton, C., et al. 2002, AJ, 123, 485

Theuns, T. et al. 2002, ApJ, 574, L111

Tittley, E. R. & Meiksin, A. 2007, MNRAS, 380, 1369

Trammell, G. B., Vanden Berk, D. E., Schneider, D. P., Richards, G. T., Hall, P. B., Anderson, S. F., & Brinkmann, J., 2007, AJ, 133, 1780

Totani, T., Kawai, N., Kosugi, G., Aoki, K., Yamada, T., Iye, M., Ohta, K., & Hattori, T. 2006, PASJ, 58, 485

Véron-Cetty, M.-P. & Véron, P. 2006, A&A, 455, 773

White, R. L., Becker, R. H., Fan, X., & Strauss, M. A. 2003, AJ, 126, 1

Wyithe, J. S. B. & Loeb, A. 2003, ApJ, 586, 693

Wyithe, J. S. B., Bolton, J. S., & Haehnelt, M. G. 2008, MNRAS, 383, 691

York, D. G. et al. 2000, AJ, 120, 1579

Zheng, W. et al. 2004a, ApJ, 605, 631

Zheng, W., Chiu, K., Anderson, S. F., Schneider, D. P., Hogan, C. J., York, D. G., Burles, S., & Brinkmann, J. 2004b, AJ, 127, 656

Zheng, W. et al. 2005, in Probing Galaxies through Quasar Absorption Lines, Proceedings IAU Colloquium 199, ed. P.R. Williams, C. Shu, & B. Ménard, (Cambridge: Cambridge Press), 484

Zheng, W. et al. 2008, $\mathrm{ApJ},\,686,\,\mathrm{in}$ press

This preprint was prepared with the AAS LATEX macros v5.2.

Table 1. Catalog of Candidate Far-UV-Bright SDSS/GALEX Quasars

Name	RA (J2000)	Dec (J2000)	Redshift	z-band (mag)	$ NUV flux (10^{-17})^{a} $	FUV flux $(10^{-17})^{a}$	Insp. ^b	Obs. ^c
SDSSJ000303.35-105150.7	0.763963	-10.864074	3.65	19.00	0.803	3.209	6	0
SDSSJ000316.39-000732.4	0.818289	-0.125675	3.17	19.99	3.218		0	0
SDSSJ001632.44+001421.6	4.135159	0.239336	3.33	20.04	2.449		0	0
SDSSJ001641.17+010045.3	4.171557	1.012579	3.05	19.28		5.232	1	0
SDSSJ003420.62-010917.3	8.585921	-1.154819	2.85	20.05	1.903	1.849	0	0
SDSSJ003930.32+001754.2	9.876321	0.298402	2.90	20.00	0.534		0	0
SDSSJ004323.43-001552.6	10.847631	-0.264620	2.80	18.14	7.721		8	0
SDSSJ005401.48+002847.8	13.506173	0.479941	3.41	19.80	4.985		3	0
SDSSJ005653.26-094121.9	14.221906	-9.689411	3.25	19.77	3.144	3.103	0	1

Note. — Excerpt of table. Full version available online in machine-readable format.

^bThe numeric inspection flag denotes possible problems with the object. The individual values are: 1 for a very near neighbor in the SDSS image, 2 for a probable LLS or DLA in the SDSS spectrum, 4 for a BAL, and 8 for a possible BAL. These individual flags are additive for a given object (e.g., 6 denotes a BAL with an LLS or DLA).

^cThe observation flag is 0 if the object has not been observed with *HST*, 1 if it has been observed with FUV (to near 304Å rest) spectroscopy through *HST* cycle 16, and 2 if it has been observed less conclusively, i.e., NUV spectroscopy, UV imaging, or pre-COSTAR observation.

 $^{^{\}rm a}$ erg s⁻¹ cm⁻² Å⁻¹, from GALEX

-24

Table 2. Catalog of Candidate Far-UV-Bright (non-SDSS) VCV/GALEX Quasars

Name	RA (J2000)	Dec (J2000)	Redshift	$ m V^a \ (mag)$	NUV flux $(10^{-17})^{b}$	FUV flux $(10^{-17})^{b}$	Obs. ^c
TEX0004+139	1.7396	14.2628	3.2	19.90	4.73		0
CXOMPJ00184+1629	4.6125	16.4831	2.828	R21.27	0.37		0
CXOMPJ00189+1629	4.7288	16.4978	2.95	R21.78	0.88		0
Q0016-3936	4.7992	-39.3278	3.	*19.79	25.05	38.29	0
2QZJ002416-3149	6.0675	-31.8289	2.846	*20.24	4.44		0
Q0023-4013	6.5912	-39.9514	3.	*19.64	3.86		0
Q0026-3934	7.1929	-39.3050	2.91	*19.59	1.64		0
Q0027-4132	7.4904	-41.2589	2.79	*19.70	3.80		0
2QZJ003130-3033	7.8750	-30.5558	2.811	*19.16	2.13		0
2QZJ003447-3048	8.6967	-30.8033	2.785	*19.97	3.99	•••	0

Note. — Excerpt of table. Full version available online in machine-readable format.

^aV magnitude unless otherwise marked as: photographic (*), blue (B), red (R), infrared (I J K), or photographic O- or J-plates (O).

 $^{\rm b}$ erg s⁻¹ cm⁻² Å⁻¹, from GALEX

 c The observation flag is 0 if the object has not been observed with HST, 1 if it has been observed with FUV (to near 304Å rest) spectroscopy through HST cycle 16, and 2 if it has been observed less conclusively, i.e., NUV spectroscopy, UV imaging, or pre-COSTAR observation.

Table 3. Quasars/Sightlines with Confirming ACS Reconnaissance UV Spectra

Name	RA (J2000)	Dec (J2000)	Redshift	NUV flux $(10^{-17})^{a}$	FUV flux (10 ⁻¹⁷) ^a	Exp. Time ^b (s)	Obs. Date	He II Ly α break
SDSSJ005653.26-094121.9	14.221906	-9.689411	3.25	3.15 ± 0.70	3.10 ± 0.91	3200	2007 Jul 18	?
SDSSJ013900.79-084720.6	24.753291	-8.789060	3.13		4.92 ± 0.95	4240	$2007~\mathrm{Jul}~19$	yes
SDSSJ080856.19+455006.8	122.234134	45.835213	3.15	0.58 ± 0.25	4.4 ± 1.3	4350	2007 Dec 3	no
SDSSJ094102.52+560706.6	145.260480	56.118488	3.79	1.34 ± 0.82		3630	$2007~\mathrm{Apr}~15$	yes
SDSSJ100610.55+370513.9	151.543968	37.087186	3.20	16.3 ± 2.4	6.1 ± 2.9	4300	2007 Nov 10	yes
SDSSJ100745.90+472321.1	151.941266	47.389197	3.41	2.6 ± 1.1	8.2 ± 3.4	4350	$2007~{\rm Dec}~19$	yes
SDSSJ100956.05+391718.4	152.483550	39.288447	3.83	$5.3 \pm 1.9^{\rm c}$		3200	$2007~\mathrm{Nov}~29$	yes
SDSSJ113721.72+623707.2	174.340509	62.618667	3.78	$4.5 \pm 2.6^{\rm c}$		3200	2007 Oct 29	yes
SDSSJ131914.20+520200.1	199.809186	52.033356	3.90		10.4 ± 4.2	3200	2007 Nov 9	?
SDSSJ144250.12+092001.5	220.708836	9.333762	3.53	5.4 ± 1.2		3200	$2007~\mathrm{Mar}~12$	yes
SDSSJ220040.92+000832.2	330.170480	0.142289	3.13	6.31 ± 0.53	11.0 ± 1.2	4240	$2008~\mathrm{Jun}~19$	yes
SDSSJ225117.80-085722.8	342.824147	-8.956327	3.12	5.52 ± 0.39	11.5 ± 1.6	4280	$2007~\mathrm{May}~13$	yes

 $^{^{\}rm a}$ erg s⁻¹ cm⁻² Å⁻¹, from *GALEX*

^bSome quasars had one or two particularly noisy or misaligned sub-exposures. Our analysis does not use these sub-exposures, nor have they been included in these tabulated exposure times.

^cFlux from *GALEX* GR1, since this source is not in GR2/GR3.

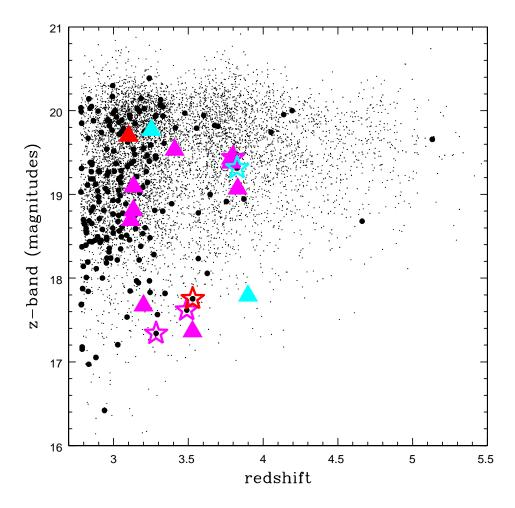


Fig. 1.— A portion of the redshift-magnitude diagram for SDSS quasars (smaller black points). There are many SDSS quasars of potential interest for helium absorption studies, e.g., with 7800 considered herein at z>2.78. The two hundred SDSS/GALEX matches cataloged here in section 2 as higher-confidence far-UV-bright quasars are highlighted as medium, filled black circles. (The symbols in color denote quasars having UV verification spectra, e.g., in anticipation of comparisons with Figure 3 and related discussion in the later sections of the text; the color-symbol coding here is the same as detailed in the Figure 3 caption).

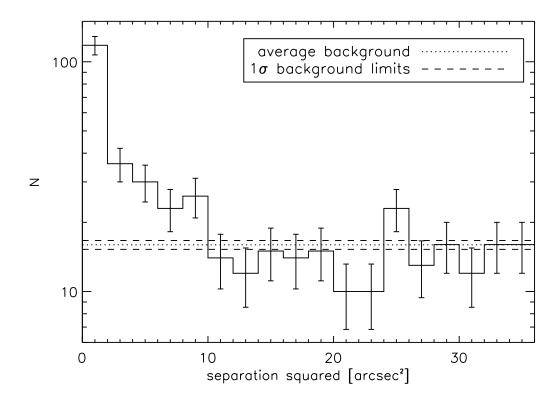
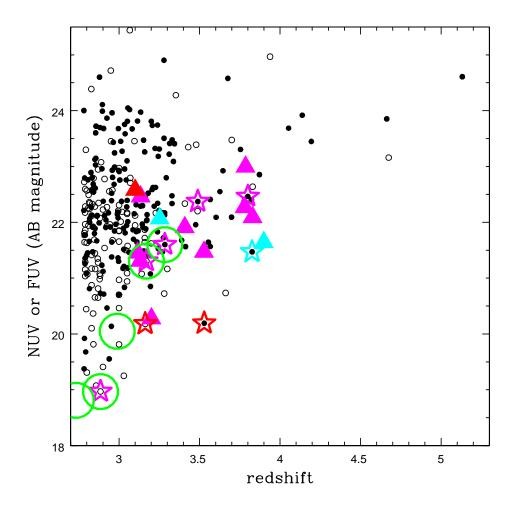


Fig. 2.— SDSS-GALEX source separation, with the background spurious match rate shown. The histogram shows the 419 $r \leq 6''$ matches, while the error bars are simply \sqrt{N} Poisson noise for each bin.



Redshift/UV-magnitude diagram for our 200 higher-confidence far-UV-bright quasars at z > 2.78 from SDSS (medium, filled black circles), and the 112 similar cases derived from VCV (Véron-Cetty & Véron 2006) quasars (medium, open black circles). Where there is a UV detection in only one of the two GALEX passbands, we plot the relevant associated AB magnitude, NUV or FUV as appropriate; for cases detected in both FUV and NUV bandpasses we plot the GALEX AB magnitude of the brighter of the two. The large triangles depict the 12 HST/prism-observed SDSS/GALEX quasars thus far confirmed as bright in the far-UV restframe (including two found only in GR1); magenta triangles depict the 9 whose HST prism spectra confirm them as excellent new clean sightlines, cyan triangles are 2 cases which may be absorbed just above the He II break and require further UV spectroscopic scrutiny, and the red triangle shows one case where our prism spectra already convincingly show strong and sharp absorption significantly redward of the He II break. For comparison, the open starred symbols show the data for the previously published confirmed or strongly suspected He II quasars; the color coding is the same as for the triangles. Large green circles denote the 5 He II quasars with extant very high-quality (in both resolution and S/N) UV spectra.

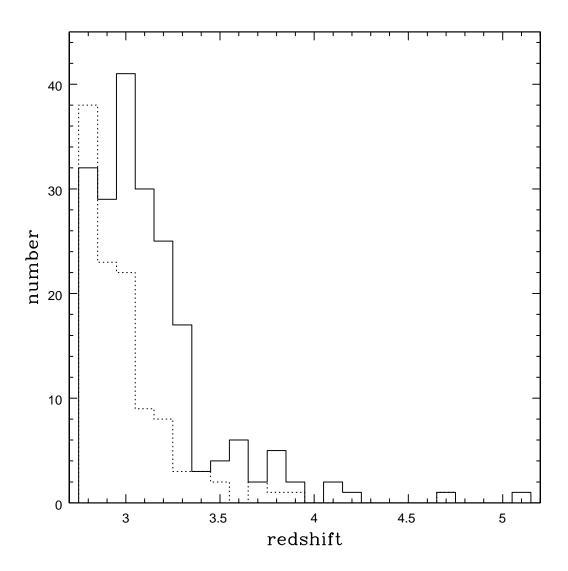


Fig. 4.— Redshift distributions of likely far-UV-bright quasars from GALEX GR2/GR3 and SDSS DR5/DR6 (solid line), or VCV (dotted line) quasars (Véron-Cetty & Véron 2006) at z>2.78.

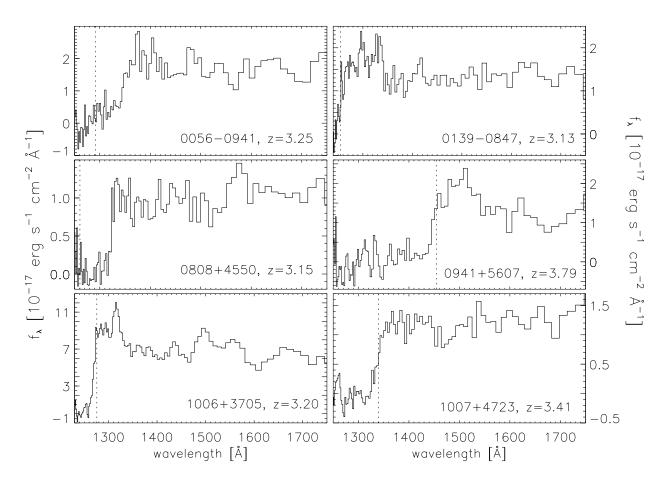


Fig. 5a.— ACS spectra for the first 6 objects in Table 3. The vertical dotted line shows the anticipated position of He II Ly α for the quasar redshift. Instrumental resolution is about 2 bins.

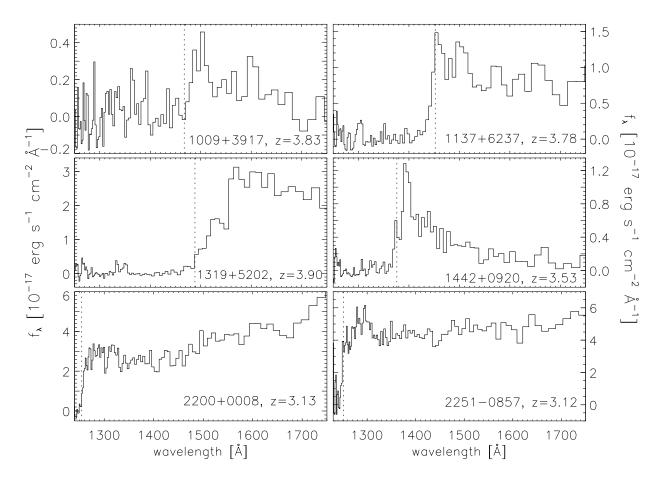


Fig. 5b.— ACS spectra for the last 6 objects in Table 3. The vertical dotted line shows the anticipated position of He II Ly α for the quasar redshift. Instrumental resolution is about 2 bins.

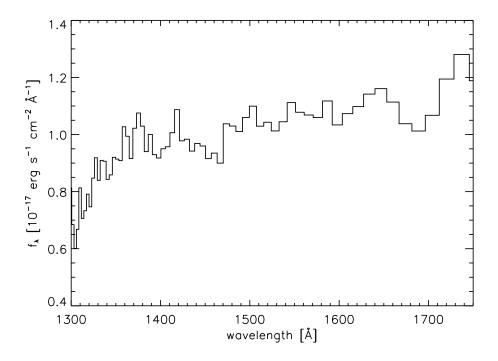


Fig. 6.— Seven of our UV prism spectra coadded/stacked in the instrument (observed) frame, weighted by flux. To obtain coverage of much of the wavelength range, the included objects are limited to those at lower redshift, z < 3.5 (He II Ly α at $\lesssim 1350 \text{Å}$). The slightly red slope is largely attributable to a single object, 2200+0008.